Mem. Fac. Sci. Shimane Univ.,
27, pp. 31–43 Dec. 27, 1993

En Echelon Arrangement of Rifting Faults in Analog Experiments

Hiroaki KOMURO* and Masashi TANIGAWA**

*Department of Geology, Faculty of Science, Shimane University, Nishikawatsu, Matsue 690, JAPAN
**Kyushu Branch, OYO Corporation, Ijiri 2-21-36, Minami-ku, Fukuoka 816, JAPAN

(Received September 6, 1993)

Experimental configurations fall into two groups; rifting associated with previous uplift (Model U) and rifting following lithospheric extension (Model E). The tests of Model U were carried out on a rubber sheet pushed up by a motor-driven block, while the tests of Model E were achieved on the conveyer belts of cloth spread to both sides.

Results of the model experiments are summarized as follows: The crustal uplift (Model U) produces a narrow rift zone consisting of faults arranged in en echelon of two orders. The first order arrangement is composed of minor faults each of which strikes in the direction of the uplift axis. Right- and left-handed en echelon faults are cyclically alternated and they develop asymmetrically with respect to the rift axis, so that they evolve into a sigmoidal fault. This sigmoidal fault is an element of the second order en echelon arrangement. The rift floor is tilted due to asymmetrical growth of boundary faults. The spreading of the crust (Model E) produces a wide rift floor bounded by meandering faults. The second order en echelon arragement is not observed in Model E.

Introduction

It is controversial whether or not mantle upwelling causes crustal uplift before rifting. According to Bott (1981), most of the continental rifting occurs in regions of crustal doming or plateau uplift. Seidler and Jacoby (1981) and Bridwell and Potzick (1981) pointed out that diapiric rise of asthenosphere causes the rifting because of the upper mantle anomaly beneath many rift zones. Girdler (1983), however, mentioned that the lithospheric thinning and hot material rising from the asthenospere are consequences of extensional rifting. Artemjev and Artyushkov (1971) also mentioned that collapse along the crestal line of a large crustal arch cannot cause the rift-valley formation.

Rifting mechanisms have been divided into two groups (Şengör and Burke, 1978; Turcotte and Emerman, 1983). The first group comprises an active mechanism, which is governed by upwelling of a convective mantle plume and consequently associates with pre-rifting uplift, whereas the second mechanism is characterized by passive rise of the asthenosphere due to the lithospheric extension and thinning.

Rifting mechanism has been studied by many authors using scale model experiments and numerically analytical methods (H. Cloos, 1939; E. Cloos, 1968; Bridwell and Potzick, 1981; Neugebauer and Temme, 1981; Ricke and Mechie, 1989; McClay and Ellis, 1987). However, most of their simulations were restricted to two-dimensional problems.

Yairi (1974) found that faults in the East African Rift System are arranged in en echelon. He inferred that this fault pattern was produced by oblique extension with respect to the rift axis. Komuro and Fukushiro (1989) explained that en echelon tensile gashes are arrayed perpendicularly to the direction of the maximum tensile stress. Fujita (1982) suggested that en echelon arrangement is the initial pattern of all fractures even if they have no lateral displacement. However, many workers generally believe that en echelon fractures originate in Riedel shear above a basal wrench fault. Less attention has been directed to en echelon arrangement of rifting fractures.

Scale model experiments provide analogical speculations on dynamic models, though it is not always fit for quantitative analyses because of material restriction. The authors carried out analog model experiments of en echelon faulting of dip-slip type and found that these faults are caused by pure extension or anticlinal uplift without strike-slip components.

Experimental Setup

Rifting was caused experimentally by placing a clay cake over rigid basement blocks. Model similarity is described as

$$\sigma_r = \rho_r\, g_r\, l_r$$

whrtr σ_r, ρ_r, g_r and l_r are model ratios of stress, density, gravity acceleration and length, respectively. Dynamical scaling is satisfied by use of wet clay which has very low visco-plastic condition (Kodama *et al.*, 1974) under the condition of $l_r = 0.5 \times 10^{-5}$. The model sizes were 30×30 cm square and 5 cm thick. Accordingly, this model equals $60 \times 60 \times 10$ km in real scale, which represents the Earth's uppermost crust.

Two experimental configurations were tested. In the first one, Model U, rifting following crustal doming without horizontal extension is simulated. The experimental apparatus of Model U is shown schematically in Fig. 1. It is made up of a rubber sheet 2 mm thick placed on a central basement block which is allowed to move upward by a motor-driven shaft with respect to the fixed blocks. Anticlinal deformation and rifting are achieved in the overlying clay cake by the differential movement of blocks as transmitted through the rubber sheet. The uplift rate of the central block is 4.2×10^{-2} (Model U-1) and 3.3×10^{-1} (Model U-2) mm/sec (Table 1). The uplift attains 25 mm. Although this uplift value may be out of scale, such an exaggerated model can visibly boost fault displacements. Accordingly, the quantitative relationship between the model and geologic structures, e.g. values of fault displacements and dip angles, are not

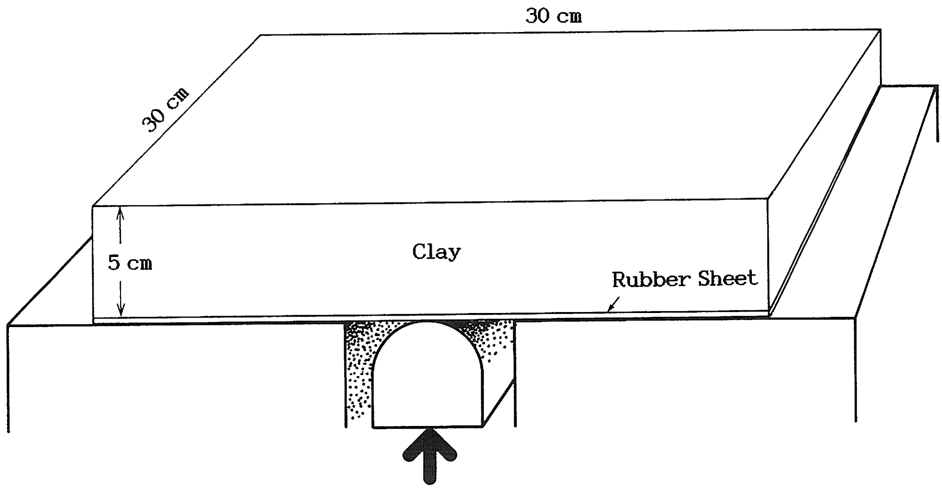

Fig. 1. Simplified sketch of experimental apparatus used for Model U. A motor-driven central block anticlinally pushes up a clay cake (30×30×5 cm) through a rubber sheet.

Table 1. Experimental models and displacement rates

	Model Code	Displacement rate (mm/sec)
Uplift Model	U-1	4.2×10^{-2}
	U-2	3.3×10^{-1}
Extension Model	E	$2\times(5.0\times10^{-3})$

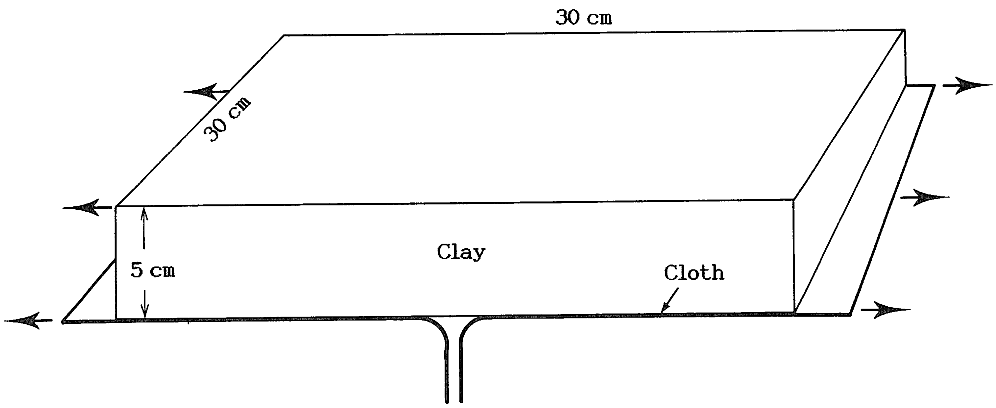

Fig. 2. Simplified sketch of experimental apparatus used for Model E. A clay cake is spread by motor-driven conveyer belts of cloth.

similar. However, we can compare the fault patterns between model facturing and geologic structures.

In the second group, Model E, extensional rifting without doming is simulated. The apparatus is shown in Fig. 2. Conveyer belts of cloth are spread from the center toward both sides at constant rates of $2\times(5.0\times10^{-3})$mm/sec (Table 1). The boundary between the clay cake and the belts is "welded", namely it has no interlayer slip. The spreading of the clay cake is focused along the linear zone where the belts move apart.

Extreme thinning of the lithosphere, a simultaneous rise of the asthenospere, and the relation between rifting and volcanism are not simulated in the authors' experiments.

Results

Model U

Figures 3–5 show the results of Model U. The progressive uplift produces short faults of dip-slip type on the model surface. These faults are oriented to the direction of the uplift axis and arranged in en echelon pattern. Right- and left-handed arrangements alternate cyclically, so that these faults form a meandering zigzag pattern (Fig. 3). These faults link together to become a curved major fault with shear senses reverse across the uplift axis (Fig. 4). No linear major fault is formed. These rifting faults

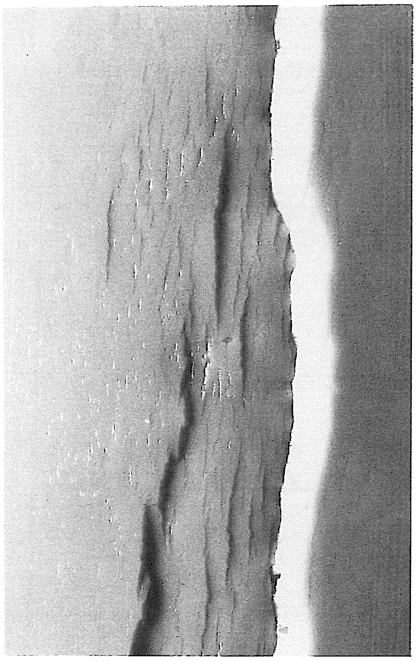

Fig. 3. Fractures developed in Model U. The long side of this photograph is about 5 cm. Note a zigzag pattern of faults which originate in alternative en echelon patterns of right- and left-handed array. This rift consists of a large-normal meandering fault and minor step faults with opposed senses.

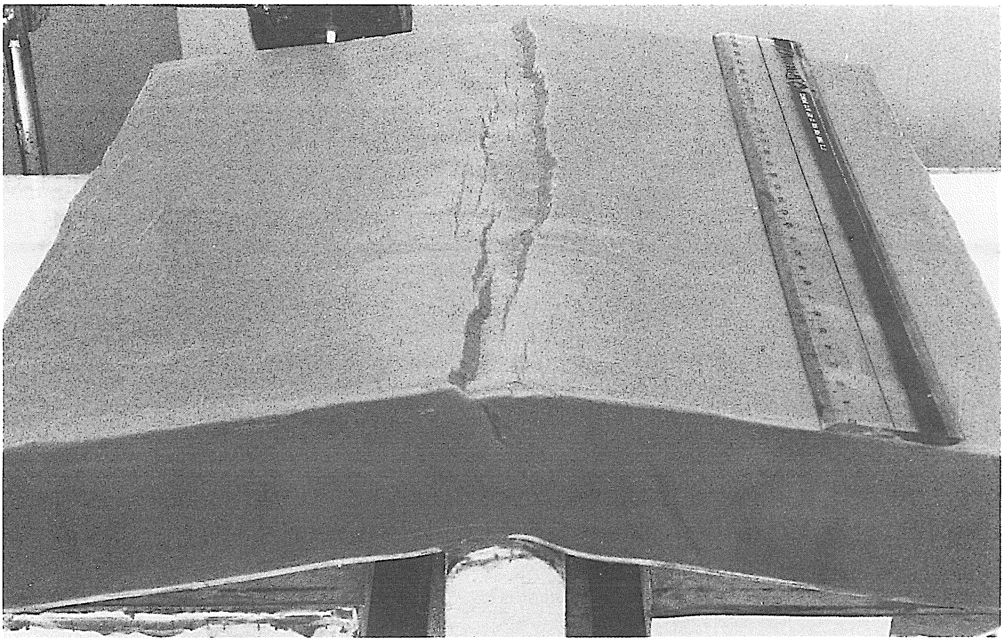

Fig. 4. Model U-1. The uplift rate is 4.2×10^{-2} mm/sec. Fault development is not symmetrical. A normal fault shown in this side crosses the uplift axis and transfers to the fault in the opposite side. Dip angles of the faults are convex-upward.

emerge at the surface and propagate downward with convex upward.

The development of rifting faults is not symmetric with respect to a rift axis. The faults on the opposite side of the sigmoidal major fault consist of poorly developed minor step faults. This asymmetrical development of the faults causes tilting of the rift floor. In the ideal case, rifting faults would be composed of conjugate shear sets which allow a wedge-shaped fault block to sink symmetrically. Only one of the conjugate shear sets seems to develop in the model because of an inhomogeneous concentration of stresses.

In Model U-2 (a high displacement-rate model; Fig. 5), more faults develop than in model U-1. Brittle behavior may be enhanced by high displacement rate. The low displacement-rate seems to allow the stress concentration along a few faults and seems to give these faults enough time to grows. Nevertheless asymmetrical growth of faults are observed in both cases.

The curved fault at top-right of this photograph seems to transfer to the fault at center-left of the photo. The center-right and bottom-left faults are also continuous. One set of the curved faults with opposite senses is defined as a sigmoidal fault. The sigmoidal faults overlap each other, so that they forms a second set of en echelon faults arrayed along the uplift axis (Fig. 5). The fault system of Model U is schematically

Fig. 5. Model U-2. The uplift rate is 3.3×10^{-1} mm/sec. A quarter wavelength of two sigmoidal faults overlap one another. The width of the rift is variable.

shown in Fig. 6.

The boundary condition at the vertical sides of the model might affect the growth of the faults. If the fault pattern were controlled by the vertically cut sides, a regular

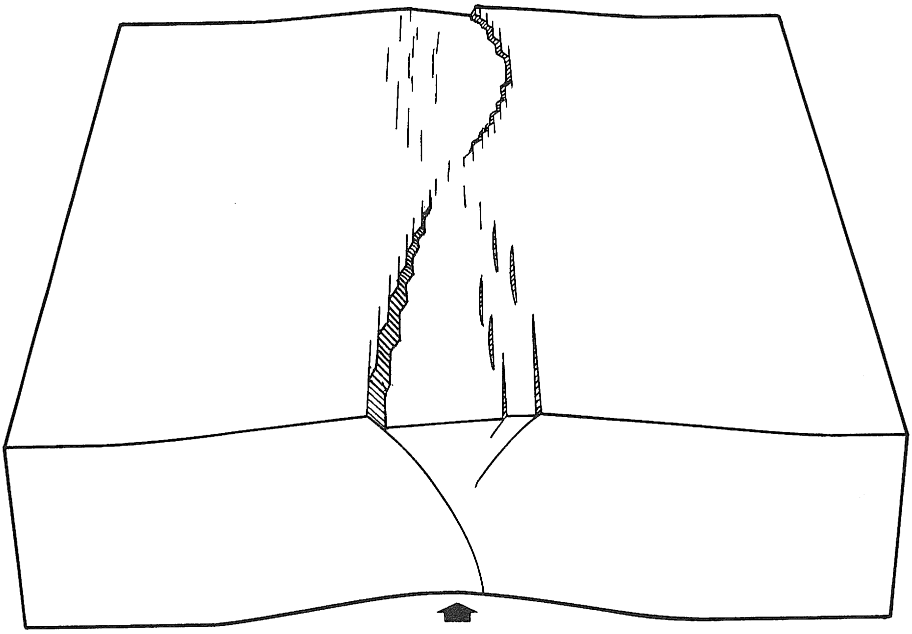

Fig. 6. Schematic illustration of Model U. Short normal faults are arrayed in the first order en echelon arrangement. These faults are linked together to become a sigmoidal major fault, of which sense is reversed across the uplift axis, and of which dip angles show convex-upward.

relationship between the signoidal fault and both ends of the model would have been observed, and the wavelength of the sigmoidal fault would have been constant. Comparing Model U-1 and U-2, any regular relationship between the sigmoidal fault and the model boundary can not be found. The boundary effect along the vertical sides of the model is out of relation to the faulting of the model rifts.

Model E

Figure 7 shows the results of Model E. Spreading of the conveyer belts causes the necking of the overlying clay cake. Planar faults at the basal-spreading center are initiated first and propagate obliquely upward. These faults are only slightly concave-upward. Short normal faults emerge at the model surface as soon as the faulting extended from the basal-spreading center reaches the surface. The rift floor is wider than that in Model U. These short faults are oriented to the uplift axis and arranged in en echelon pattern similar to those in Model U. Right- and left-handed arrangements altemated cyclically, so that these faults strike meanderingly. However, the sigmoidal faults as observed in Model U are not produced, probably because the width of the rift floor is so large that the meandring boundary faults do not cross the rift axis. Consequently, the second order arrangement of en echelon is not observed.

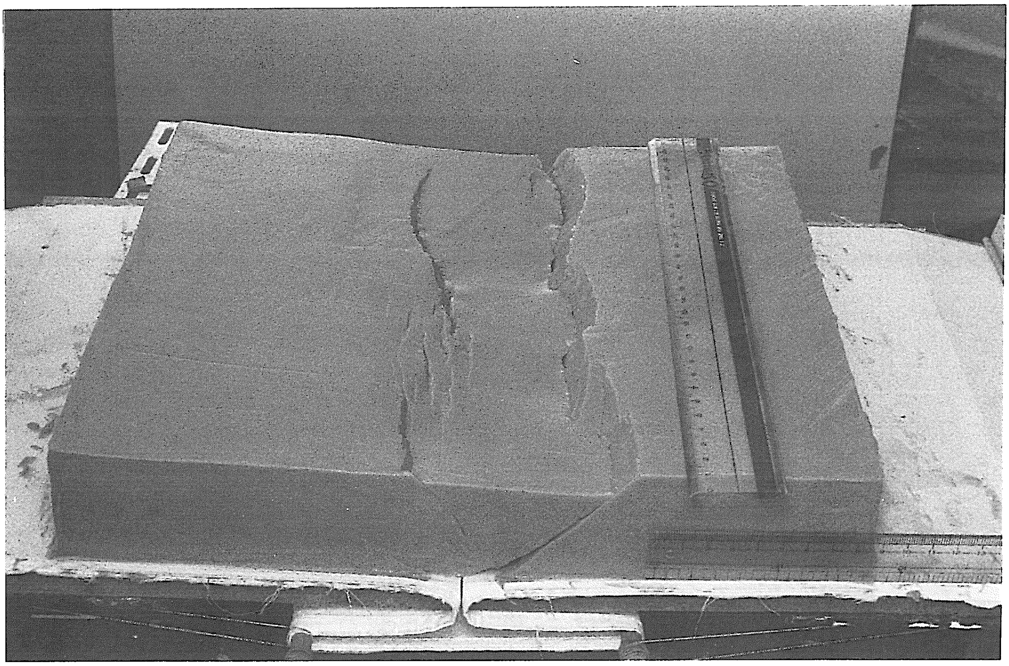

Fig. 7. Model E. The extension rate is $2\times(5.0\times10^{-3})$ mm/sec. Note a marginal winding fault and step faults. Faults in the vertical side of the model are almost linear or weakly concave-upward.

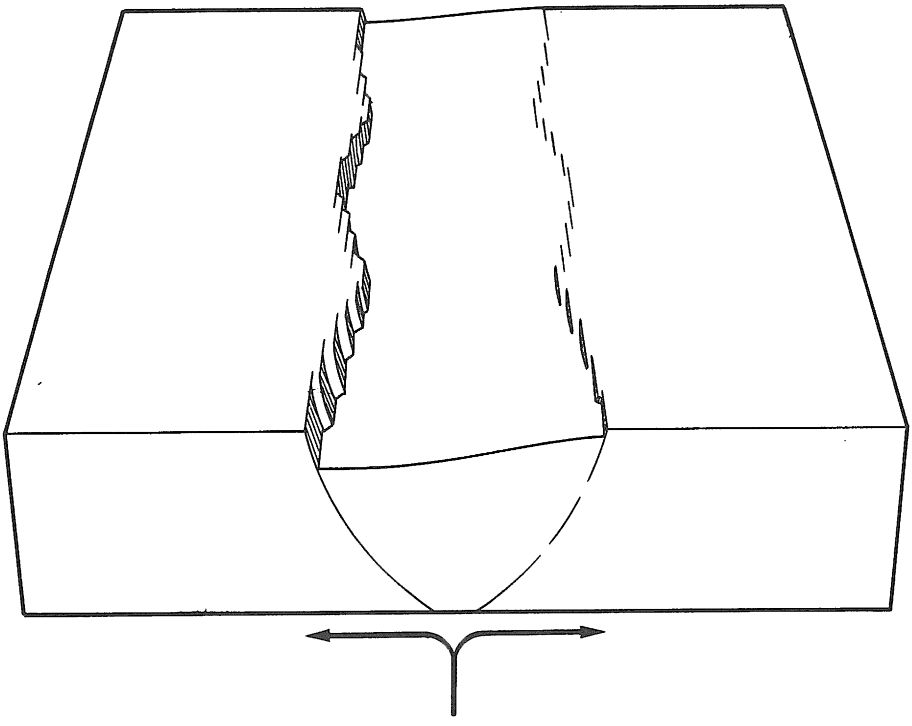

Although the spreading rate is symmetrical on both sides, the displacements along the faults are not. This asymmetry is particularly conspicuous in the model with low displacement rate. Both of the marginal faults of the rift grow asymmetrically, so that at the surface the rift floor tilts toward the larger fault.

The fault system of Model E is schematically drawn in Fig. 8.

Discussion

Two orders of en echelon arrangement are observed in Model U. The first orger

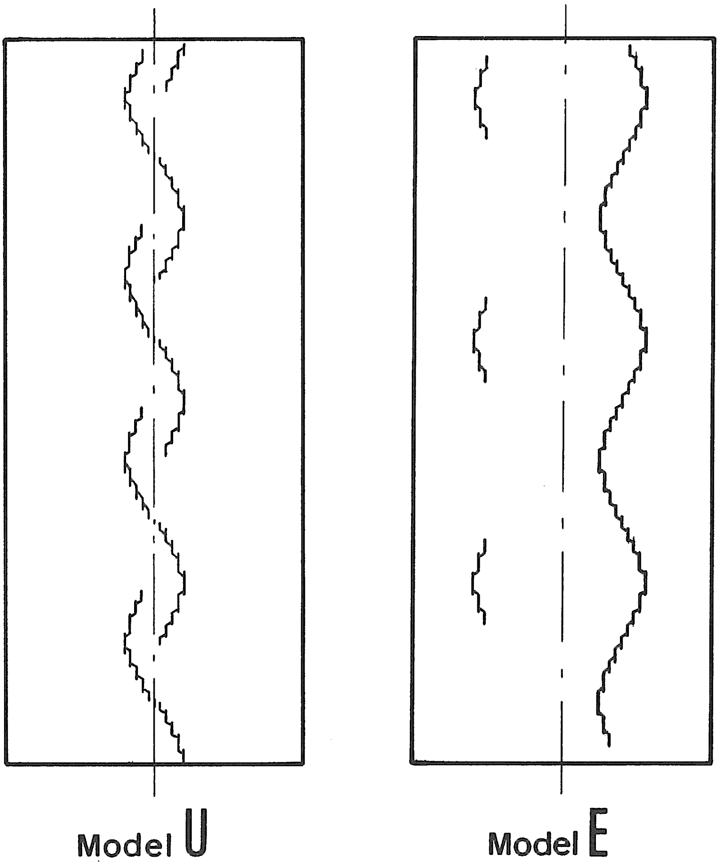

Fig. 9. Simplified patterns of en echelon faults in Model U and E. Sigmoidal faults are arrayed for en echelon of the second order along the rift axis in Model U, whereas only the first order arrangement develops in Model E.

Fig. 8. Schematic illustration of Model E. Short normal faults show en echelon arrangement of the first order, which link together to become the winding faults. The marginal faults are almost linear or weakly concave-upward. The wide rift floor inclines to the larger marginal fault.

arrangement consists of short faults each of which strikes in the direction of the uplift axis. The right-handed arrangement cyclically alternates with the left-handed one, so that the rifting faults become meandering faults and evolve into sigmoidal faults (Fig. 9). These sigmoidal faults form the second order arrangement along the uplift axis. Each element of the first order arrangement strikes the anticlinal axis, whereas the element of the second order is obliquely oriented with respect to the direction of the axis. However, the second order arrangement is not observed in Model E.

These different patterns of rifting faults between Mocel U and E may give a criterion as to whether the uplift precedes the rifting. The pre-rifting uplift should produce a narrow rift zone composed of en echelon sigmoidal faults, whereas basal spreading of the upper curst should produce a wide rift bounded by meandering faults.

Artyushkov (1987) designated 'graben' as a narrow rift collapsed by key-stone effect without extension and 'rift' as a wide rift accompanying a large extension of the lithospere. The authors infer from Model U that the narrow rift is produced only by the pre-rifting uplift. The width of the spreading rift is larger than the thickness of the extending brittle layer, because the boundary faults of this type begin from the basal spreading center and grow upward conjugately.

Illies (1981) observed a zigzag margin and en echelon array of intra-rift faults in the Rhine Graben and concluded that this pattern is controlled by the pre-existing structure and post-rifting lateral movement. Elmohandes (1981) simulated a lateral rift/rift offset of the Rhine Graben by setting up a transform fault of the basement. Tokuda (1926) and Lee (1929) inferred that en echelon arrangement of fold axes in island arcs are produced by laterally momental forces. Yairi (1974) performed sand box experiments and suggested that oblique extension produces tension cracks arranged in en echelon. However, Model E and especially Model U show that the en echelon faulting is caused by the rifting without any strike slip component.

In many continental rifts, the width of rifts are variable, and the rifting faults are not linear. The Baikal rift seems to consist of asymmetric sigmoidal faults (Fig. 10) (Zorin, 1981). The eastern and western rifts of the East African Rift System go round Lake Victoria in sigmoidal rifts. Faults in the Kenya Rift are also sigmoidal (Logatchev *et al.*, 1983). A rift zone from the East African Rift System through the Red Sea to the Dead Sea looks like a large continuous sigmoidal rift zone. Girdler (1983) concluded that the lithospheric thinning of the East African Rift System is a consequence of extensional rifting. However, the African plate is surrounded by the ocean ridges and does not suffer any slab-pull force. These continental rifts may be formed by the upwarping of the crust-lithosphere caused by the asthenosperic diapirs emplaced at various levels of the brittle lithosphere.

Morley (1988) and Morley *et al.* (1990) defined a transfer zone between two major faults and classified rift geometries into three basic types; conjugate convergent, conjugate divergent and synthetic ones. The approaching-convergent transfer zone of Morly *et al.* (1990) is identified with the sigmoidal fault in our Model U. Their

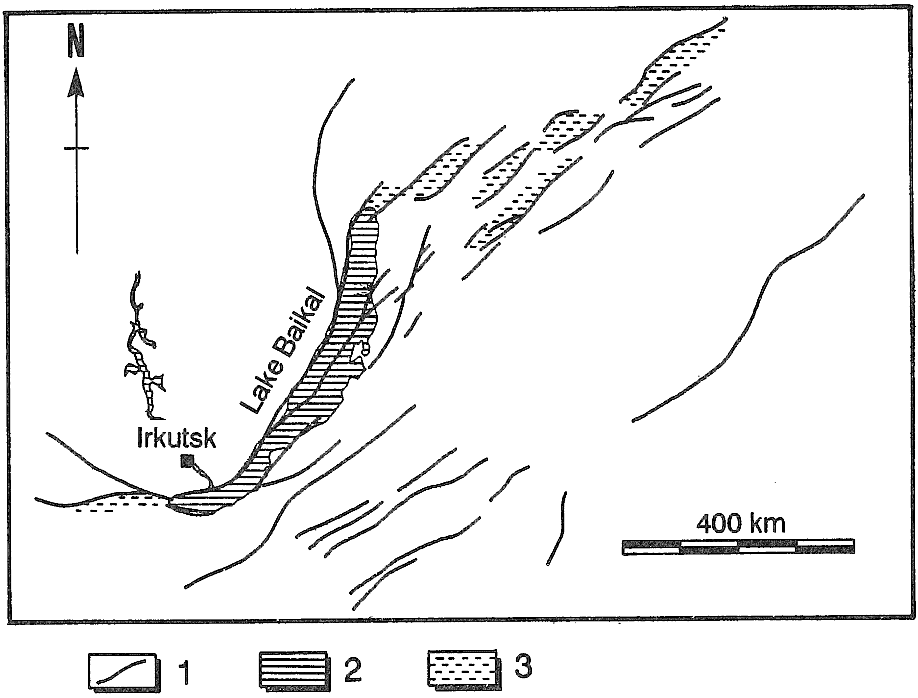

Fig. 10. Structural map of the Baikal rift zone (simplified from Zorin, 1981).
1: faults, 2: Lake Baikal, 3: Cenozoic sedimentary rocks.

overlapping-convergent transfer zone is also observed in our Model U. The transfer zones in conjugate convergent and divergent types across a graben axis. These types of rifting may be controlled by the crustal doming.

Conclusions

Clay models reveal different fracture patterns for uplift-rifting and extensional rifting. The analogy from the models is drawn as follows:

The crustal uplift produces a narrow rift consisting of faults with two order en echelon arrangements. The first order arrangement consists of minor faults striking the uplift axis, whereas the element of the second order arrangement consists of a sigmoidal fault. The sigmoidal fault is a chain of the minor faults arranged in en echelon of the first order. Fault development is asymmetrical with respect to the uplift axis.

The spreading of the crust produces a wide rift bounded by meandering faults. The fault development is asymmetrical so that the rift floor is tillted.

Acknowledgments

We are grateful to Dr. Yukinori Fujita for useful advice. We also thank Dr. Takao Yano of Hiroshima University, Dr. Keiichi Nishimura of Kyoto University and Dr. Yoshihiro Sawada of Shimane University for valuable discussions during the development of this work.

References

Artemjev, M. E. and Artyushkov, E. V., 1971. Sructure and isostasy of the Baikal rift and the mechanism of rifting. *Jour. Geophys. Res.*, **76**, 1197–1211.

Artyushkov, E. V., 1987. Rifts and grabens. *Tectonophysics,* **133**, 321–331.

Bott, M. H. P., 1981. Crustal doming and the mechanism of continental rifting. *Tectonophysics,* **73**, 1–8.

Bridwell, R. J. and Potzick, C., 1981. Thermal regimes, mantle diapirs and crustal stresses of continental rifts. *Tectonophysics,* **73**, 15–32.

Cloos, H., 1939. Hebung—Spaltung—Vulkanismus. *Geologische Rundshau,* **30**, 404–525.

Cloos, E., 1968. Experimental analysis of Gulf Coast fracture pattems. *Amer. Assoc. Potrol. Geol.,* **52**, 420–444.

Elmohandes, S. E., 1981. The central European graben system: rifting imitated by clay modeling. *Tectonophysics,* **73**, 69–78.

Fujita, Y., 1982. On the Island Arc Disturbance. *Monogr. Assoc. Geol. Collab. Jpn.,* 24, 1–32.*

Girdler, R. W., 1983. Processes of planetary rifting as seen in the rifting and break up of Africa. *Tectonophysics,* **94**, 241–252.

Illies, J. H., 1981. Mechanism of graben formation. *Tectonophysics,* **73**, 249–266.

Kodama, K., Suzuki, Y., Ogawa, G. and Maruta, Y., 1974. On the internal structure of box-shaped folds. *Rep. Geol. Sur. Jpn.,* No. 250-2, 121–143.*

Komuro, H. and Fukushiro, H., 1989. Three dimensional stress analyses around a rising dome by means of finite element method. *Monogr. Assoc. Geol. Collab. Jpn.,* 36, 209–219.*

Lee, J. S., 1929. Some characteristic structural types in Eastern Asia and their bearing on the problem of continental movements. *Geol. Mag.,* **66**, 501–522.

Logatchev, N. A., Zorin, Y. A. and Rogozhina, V. A., 1983. Baikal rift: active or passive? —Comparison of the Baikal and Kenya rift zones. *Tectonophysics,* **94**, 223–240.

McClay, K. R. and Ellis, P. G., 1987. Geometries of extensional fault systems developed in model experiments. *Geology,* **15**, 341–344.

Morley, C. K., 1988. Variable extension in Lake Tanganyika. *Tectonics,* **7**, 785–801.

Morley, C. K., Nelson, R. A., Patton, T. L. and Munn, S. G., 1990. Transfer zones in the East African Rift system and their relevance to hydrocarbon exploration in rifts. *Amer. Assoc. Petro. Geol. Bull.,* **74**, 1234–1253.

Neugebauer, H. J. and Temme, P., 1981. Crustal uplift and the propagation of failure zones. *Tectonophysics,* **73**, 33–51.

Ricke, M. and Mechie, J., 1989. Finite element modeling of a continental rift structure (Rhinegraben) with a large-deformations algorithm. *Tectonophysics,* **165**, 81–91.

Seidler, E. and Jacoby, W. R., 1981. Parameterized rift development and upper mantle anomalies. *Tectonophysics,* **73**, 53–68.

Şengör, A. M. C. and Burke, K., 1978. Relative timing of rifting and volcanism on Earth and its tectonic implications. *Geophys. Res. Lett.,* **5**, 419–421.

Tokuda, S., 1926/1927. On the echelon structures of Japanese archipelagoes. *Jpn. Jour. Geol. Geog.,* **5**, 41–46.

Turcotte, D. L. and Emerman, S. H., 1983. Mechanism of active and passive rifting. *Tectonophysics,* **94**, 39–50.

Yairi, K., 1974. En echelon pattern of the East African Rift system. *Africa Kenkyu,* 14, 21–46.*

Zorin, Y. A., 1981. The Baikal rift: An example of the intrusion of asthospheric material into the lithosphere as the cause of disruption of lithospheric plates. *Tectonophys.,* **73**, 91–104.

* In Japanese with English abostract